Journal of Metals, Materials and Minerals, Vol.25 No.2 pp.23-29, 2015

Effect of Ni on the Formability and Texture of Hot Rolled Weathering Steel

Gadadhar SAHOO[1]*, I. S. WANI[2], S. B. KUMAR[3], Balbir SINGH[1], Atul SAXENA[1] and R. BASU[4]

[1]R&D Centre For Iron and Steel, SAIL, Ranchi, India, 834002
[2]IIT Hyderabad, Yeddumailaram, Andhra Pradesh, India, 502205
[3]Department of Materials and Metallurgical Engineering, NIFFT, Ranchi, India, 834003
[4]Department of Mechanical Engineering, ITM University, Gurgaon, India, 122017

Abstract

Formability behavior in two grades of hot rolled low carbon weathering steel with varying nickel content i.e., SCR 1 (Fe-0.116P-0.018Ni) and SCR 2 (Fe-0.115P-0.34Ni), have been evaluated in relationship to microstructure, EBSD estimated orientation distribution function (ODF), special boundary nature, mechanical properties and formability parameters like tensile stain hardening exponent (n) and plastic anisotropy ratio (r). The alloy sample SCR 1 exhibited improved formability characteristics in terms of stain hardening exponent (n) and plastic anisotropy ratio (r). This was mainly attributed to relatively higher fraction of the ND//<111> orientation or the γ fibre texture component and increased presence of sigma 3 coincident site lattice (CSL) boundaries in SCR 1 . The γ fiber is mainly responsible for deep drawability in these materials.

Keywords : Weathering Steel, Formability, Strain hardening exponent, Plastic anisotropy ratio, Electron backscattered diffraction (EBSD), Coincident site lattice (CSL) boundaries.

DOI : 10.14456/jmmm.2015.12

Introduction

Weathering Steel (WS) is used in place of carbon steel to combat the degradation of steel by atmospheric corrosion. The characteristic of these alloys is their ability to generate rust that minimizes the corrosion level within accepted tolerance. This allows them to be used in corrosive conditions without the needs of protective coating during prolong exposure.(1)

Weathering steels (WS), also known as low-alloy steels, have carbon content less than 0.2 wt. % added with 3-5 wt. % of Cu, Cr, Ni, P, Si and Mn.(2) Alloying elements are added in varying amount to form the protective rust layer which prevents the steel from further rusting and also induce high strength in the steel.(3) These steels find use in applications which are prone to atmospheric corrosion like, warehouse, bridges, railway coaches, containers, pre-weathered steel panels, transmission towers etc.(3) In general, the corrosion behavior of the steels and alloys has been reported to depend on processing and deformation routes adopted(4), and also on microstructure and composition of the material.(5) The deformation introduces certain grain orientations that are sensitive to chemical attack. For example, ND//<110> and ND//<111> oriented (γ fiber) grains in materials have been reported in several literatures to increase the chemical resistance of many engineering materials under different corrosive environments.(5) Similarly, the presence of alloying elements can significantly alter the post processing microstructure or crystallographic texture during deformation (hot/cold) which in turn largely affects the mechanical properties in these materials. While the effect of other alloying elements like C, P, Cu etc. is well known on formability of steels, little study has been done on the effect of Ni. A proper selection of composition, microstructure with enhanced mechanical properties in a material is a pre requirement for designing of process during large scale production of these corrosion resistant components. In this study an attempt has been made to understand the formability behavior of the two steel grades with varying nickel content in presence of phosphorous.

Formability of sheet metal depends on the mechanical properties of the material.(6) The important material characteristics which determine the forming capacity of sheet metal are strength and ductility. The ductility determines the deformation in a material that can withstand without undergoing failure. In forming process, ductility generally depends on the plastic properties rather than the fracture behavior of materials.(7) It is well identified that ductile fracture occurs as a consequence of

*Corresponding author E-mail : gadadhar@sail-rdcis.com

prior localization of the deformation to form a neck. The plastic properties characterizing ductility are plastic anisotropy ratio (r) and the strain-hardening exponent (n). While plastic anisotropy ratio (r) is determined from the ratio of the strain in the width direction to that in the thickness direction, the strain-hardening exponent (n) are usually obtained from uniaxial tension tests.

Though uniaxial tensile test does not exactly imitate sheet forming, but both plastic anisotropy ratio (*r*) and the strain-hardening exponent (n) plays a role and a correlation between the two exists.[7] Both the above mentioned properties are important from two perspectives of formability of materials, e.g., in drawing operations, r is of prime importance, while n is of lesser importance. On the other hand, in stretch-forming, the opposite is true. These two properties in a specimen can be evaluated using a standard tensile test.[7]

In the present work, formability of two weathering steel sheets has been studied by uniaxial tensile loading in a mechanical testing machine. In an attempt to understand the changes in the experimentally obtained data in the two grades of alloy, microstructural characterization through electron back scattered diffraction (EBSD) techniques has been carried out. The work reports a direct correlation of mechanical properties to the initial microstructure and texture in the two grades of steel.

Experimental Procedure

Four numbers of laboratory heats of low alloy steels of 25 kg each were made using a high frequency induction melting furnace. Steel scrap of C-Mn rail steel was added to soft iron (0.001 wt. % C) to balance carbon content. In order to obtain Cr, P, Cu and Ni in the desired ranges, mother alloys of Fe-P, Fe-Cr along with Cu blocks and Ni lumps were added to the liquid steel in the furnace. Aluminium in the form of shots and wire were used for de-oxidation purpose. The melts were cast into 100mm × 100mm square ingots, which were subsequently hot rolled to plates in two stages. Details of the chemical composition of the two alloys are summarized in Table 1. SCR 1 and 2

Table 1. Chemical composition of experimental steel in wt.%

Weathering Steels	C	Si	Mn	S	P	Cr	Cu	Ni	N	A
SCR 1	0.073	0.40	0.45	0.009	0.116	0.36	0.35	0.018	0.005	0.17
SCR 2	0.072	0.38	0.44	0.007	0.115	0.36	0.35	0.34	0.005	0.17

represents alloys of low and high nickel content respectively. Flat sheet specimens for tensile tests were machined from the rolled material. The specimens as represented in Figure 1 were sectioned along 3 different directions with respect to the specimen rolling direction. The dimensions were maintained as per ASTM standards (ASTM 8M/A370).[8] These directions also corresponding to tensile axis have been generically termed as LD (longitudinal direction/rolling direction(RD)), DD (diagonal direction/45° to RD) and TD (transverse direction/ normal to RD). The testing was performed at room temperature using universal testing machine 7200 (Dak System Inc) at a strain rate of 0.001s-1. The standard tensile properties, viz., 0.2% proof stress, ultimate tensile strength (UTS) and percentage elongation (EL) were determined from the engineering stress-strain plots. The strain hardening exponent 'n' in this study was obtained by plotting log of true stain versus log of true stress using the simple power curve or Hollomon equation[1] given below and using linear regression (least square method) best-fit method considering true stress 'σ' and true strain 'ε' only for the uniform plastic deformation region[9] :

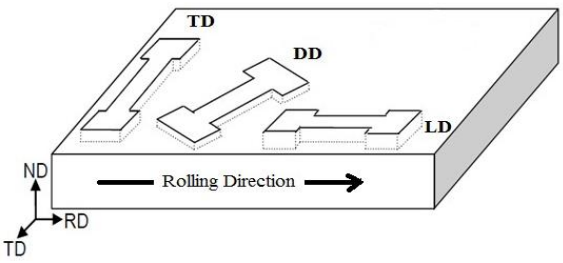

Figure 1. Orientation of the sample machined from the sheet metal for mechanical testing.

$$\sigma = k\varepsilon n \qquad (1)$$

where σ = true stress, ε = true strain, n = strain hardening exponent, K = strength coefficient.

Specimens for optical microscopy were prepared using conventional metallographic polishing routes. The grain sizes were determined by using Leica Image analyser system by E112 Planimetric method. For the electron back scattered diffraction (EBSD) analysis, samples were electropolished along rolling plane using a Struers system (Model: Polectrol) in an electrolyte of 80:20 (by volume) methanol to perchloric acid at 30 volts DC and -150C. The EBSD data acquisition was performed in a Scanning Electron Microscope (EVO MA 10, Carl Zeiss) equipped with Oxford Instruments (OI) Nordlys Max fast EBSD detector. The microscope was operated with primary electron energy at 20k eV. A step size of 1.5 μm was maintained for all the measurements performed. The OI-HKL Channel 5 software was utilized to analyze the acquired EBSD data. The ODFs were calculated from the EBSD scan using the Bunge convention.[10]

Result and Discussion

Optical Micrography

Figure 2 illustrates the light optical photo micrographs of hot rolled SCR 1 and SCR 2 consisting of ferrite-pearlite microstructure, which is typically observed for low carbon and low alloy steels. The average ASTM grain size number for the two different alloys ranges between 9.9 to 10.3, which showed little effect of Ni content on grain size.

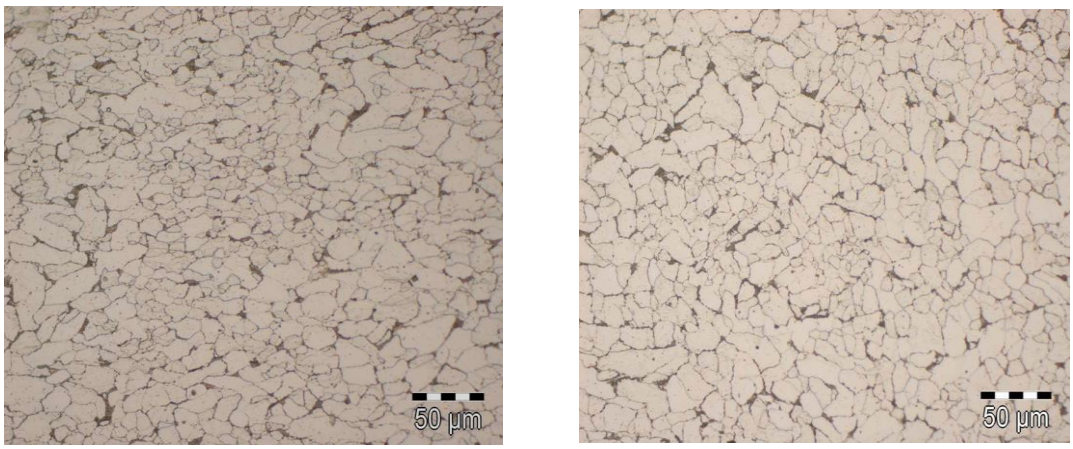

(a) (b)

Figure 2. Optical micrograph of hot rolled SCR 1 (a) and SCR 2 (b).

Mechanical properties

-Tensile properties

Tensile test were conducted for SCR 1 and SCR 2 at room temperature with the specimen axis oriented at 0°, 45°, and 90° to the rolling direction. The average values of proof strength, UTS, % elongation, strain hardening exponent (n) are provided in Table 2. The strain hardening exponent (n) in Table 2 was obtained from the log σ- log ε plot using equation (1). It is known that a material with a high strain hardening exponent, or n value, has a greater capacity for being formed (i.e., stretched or bent in a forming die) than a material with a low n value.[8] In the present work, sample SCR 1 exhibited higher average strain hardening exponent implying higher formability. The lower n value of SCR 2 steel is attributed to the presence of much higher content of Ni (0.34 %) in it than that of SCR 1 steel (0.018%). However, there was neither any particular trend nor any significant difference between the tensile properties, viz., YS, UTS and percentage elongation.

Plastic Strain ratio (r)

More insight related to formability can be obtained from the plastic anisotropy ratio (r) analysis. It is a measure of plastic anisotropy and is related to the preferred crystallographic orientations within a

Table 2. Mechanical Properties of Weathering steels

Weathering Steel	Orientation w.r.t RD (0°)	0.2% Proof Stress (MPa)	UTS (MPa)	Total elongation %	Uniform elongation %	Strain hardening exponent (n)
SCR 1	0 (LD)	439.8	534.7	15.0	7.1	0.115
	45 (DD)	418.4	525.6	13.4	8.0	0.128
	90 (TD)	435.7	520.2	15.1	7.8	0.123
Average*		428.0	526.5	14.2	7.7	0.124
SCR 2	0(LD)	422.6	503.2	15.2	9.0	0.132
	45(DD)	451.8	512.9	16.7	8.8	0.128
	90(TD)	451.4	510.7	14.4	9.4	0.132
Average*		444.4	510.0	15.7	9.0	0.130

Average X = (X1, X2 , X3 are the values of LD, DD, TD) [11]

The normal anisotropy (r) and planar anisotropy (Δr) are calculated by using the standard formulae [11] given below:

$$\bar{r} = \frac{r_0 + 2\,r_{45} + r_{90}}{4} \qquad (2)$$

$$\Delta r = \frac{r_0 - 2\,r_{45} + r_{90}}{2} \qquad (3)$$

polycrystalline metal. The resistance of a material to thinning which introduces a differential strengthening between the in-plane and through thickness direction is known as normal anisotropy value (r), and is considered as a measure of sheet metal drawability[11] while the planar anisotropy (Δr) defines the variation of flow properties in the plane of the sheet and must be kept low for reducing the earring defect during deep drawability of material.[12] As presented in Table 3, the normal anisotropy value of SCR 1 is lower (0.70) than that of SCR 2 (0.84) while the reported value for hot-rolled low-carbon steels ranges from 0.8 to 1.0.[12] However, the negative value of the planar anisotropy of SCR-1 indicates that it has lower tendency for ear formation and the combination of higher and lower Δr will provide optimal formability in contrast to the case of SCR-2.[13] Therefore, the presence of the Ni (0.34%) in SCR 2 steel influenced its formability. For further understanding, the formability characteristic of both these steels will be evaluated from the EBSD measurements in the following section.

Texture

EBSD estimated texture of two hot rolled steels shown in the orientation distribution function (ODF) plot display important BCC rolling texture components (see Figure 3). The important components are illustrated in a Φ2 = 45° section standard ODF map (Figure 3c).[14] A

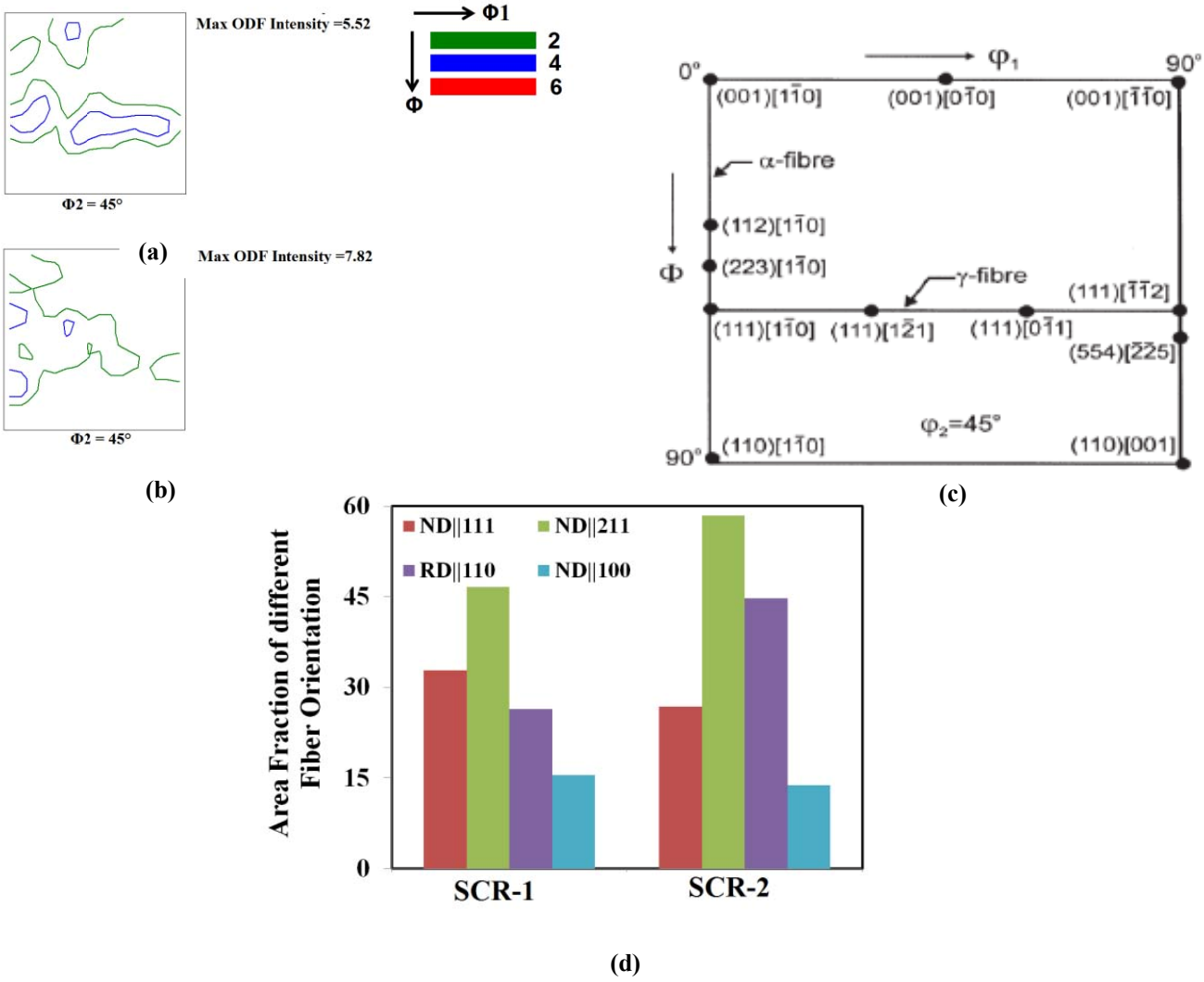

Figure 3. Φ2 = 45° section of ODF ; (a) SCR 1 and (b) SCR 2. γ fibre texture is more prominent in the sample SCR 1. ODF intensities correspond to color contours in the inset (c) standard ODF map showing important rolling texture components.[14] (d) area fractions estimated for important fibers within 10 deg tolerance.

noticeable near ND//<111> orientation or the near γ –fibre texture is clearly brought out for the sample SCR 1 with week presence of near cube orientation, {001} <100>. Though the exact origin of the γ –fibre texture in SCR 1 is not precisely understood, it appears the presence of Ni and P could have played a role in the development of γ –fibre texture. The γ –fibre component constitutes those orientations with {111} crystallographic planes parallel to the rolling plane.[14] There exists a strong correlation between texture and formability. Many of the reported work on recrystallization textures in BCC steels have shown deep drawing properties are greatly improved by the presence of high intensities and uniform distribution of the γ -fibre. Cold working followed by recrystallization annealing in BCC materials shows limited range of recrystallization textures. Recrystallization of BCC steels lead to strengthening of the γ –fiber orientation at the expense of alpha fiber.[15-17] The γ –fibre texture results from strain induced boundary migration (SIBM) where nuclei of γ –fibre grains form at the regions of high angle grain boundary.[18] Samajdar et al. have demonstrated that γ –fibre orientations between {111}<110> and {111}<112> in the cold worked state are distinct for higher stored energy which is the driving force for the growth of nuclei of γ –fibre orientations and these grains grow at the expense of other orientations. In other words a growing nuclei inherits the orientation of the parent cold worked grain. The observed patterns of γ –fibre texture during cold rolling in low carbon and ferritic steels is well established in several different works. It is usually

observed in many ferritic steels that during the stages of hot rolling in the austenitic regime no strong texture is introduced. However, for most low carbon and IF steels, the textures after complete phase transformation from austenite to ferrite resembles typical cold rolled texture.[19-21] There is still lack of understanding on the development of hot rolling textures which arise mostly during the cooling as a result of phase transformation.

Boundary nature analysis

The changes in the observed mechanical properties reported in the present study had a strong bearing on the special boundary nature. Previous researches on special boundaries, more commonly called as coincident site lattice boundaries (CSL boundaries) have shown to improve chemical, mechanical and electrical properties in several different materials.[22] CSL(Σ) boundaries are characterized by periodic arrangement of dislocations.[14] As illustrated in figure 4(c), the fraction of the Σ3 boundaries (represented as red in the grain boundary map) were highest in SCR1. Σ3 boundaries tend to minimize the grain boundary energy thereby reduces the stored energy of the material. The minimization of stored energy enables the material to plastically deform more easily or in other words formability is improved.

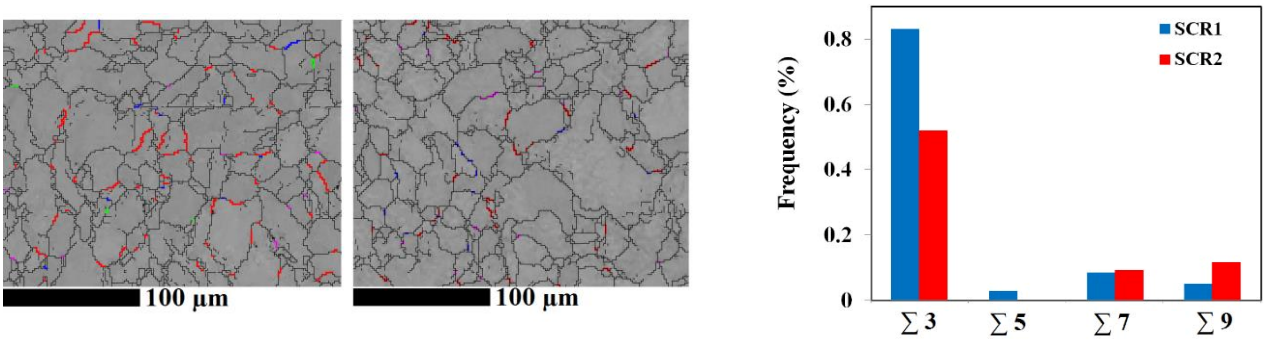

Figure 4. CSL boundary map for alloy (a) SCR 1 (b) SCR 2.
(c) relative presence of CSL (∑)boundaries for the given alloys.

Conclusions

- Two weathering grade steels, i.e., SCR 1 and SCR 2 with different Ni content were studied to evaluate mechanical properties, especially, plastic anisotropy and texture.
- Although the tensile properties of both SCR1 and SCR2 steel were not significantly different, the SCR1 steel exhibited greater degree of formability than that of SCR2 steel due to the higher value of strain hardening exponent, and lower value of Δr (negative).
- SCR 1 steel exhibited increased amount of γ –fibre texture, which is generally observed in formable grade steel. EBSD investigation also revealed higher relative presence of Σ3 boundaries in SCR 1, which will minimize grain boundary energy and improve strength and formability.
- The observed difference in the degree of formability and γ –fibre texture content in two investigated steels has been attributed to the influence of Ni content.

References

1. Kihira, H., Tanaka, M., et al. (2004). Shinnittetsu Giho. *Nippon Steel Technical Report*. **380** : 28-32.

2. Díaz, I., Cano, H., de la Fuente, D., Chico, B., Vega, J. M. and Morcillo, M. (2013). Atmospheric corrosion of Ni-advanced weathering steels in marine atmospheres of moderate salinity. *Corros. Sci.* **76** : 348-360.

3. Prasad, S.N., Mediratta, S.R. and Sarma, D.S. (2003). Influence of austenitisation temperature on the structure and properties of weather resistant steels. *Mater. Sci. Eng. A*. **358(1)** : 288-297.

4. Diaz, I., Cano, H., de la Fuente, D., Chico, B. Vega, J. M. and Morcillo, M. (2013). Atmospheric corrosion of Ni-advanced weathering steels in marine atmospheres of moderate salinity. *Corr. Sci*. **76** : 348-360.

5. Zhang, L., Szpunar, J., Basu, R., Dong, J. and Zhang, M. (2014). Influence of cold deformation on the corrosion behavior of Ni-Fe-Cr alloy 028. *J. Alloys Comp.* **616** : 235-242.

6. Banabic, D. (2000). *Formability of Metallic Materials*. Springer, New York.

7. Cada, R. (1996). Comparison of formability of steel strips, which are used for deep drawing of stampings. *J. Mater. Proc. Technol.* **60(1-4)** : 283-290.

8. ASTM E8/A370. (2015). *Standard test methods and definitions for mechanical testing of steel products.*

9. George, D. (1988). *Mechanical Metallurgy*. McGraw Hill, London.

10. Bunge, H. J. (1969). *Mathernatische Methoden der Texturanalyse*. Academic Press, Berlin.

11. ASTM E517. (2010). *Standard Method for plastic strain ratio r.*

12. Ravi Kumar, D. (2002). Formability analysis of extra-deep drawing steel. *J. Mater. Proc. Technol.* **130-131(20)** : 31-41.

13. ASM metal Handbook Vol.14 (2005). *Forming and Forging.*

14. Humphreys, F. J. and Hatherly, M. (2004). *Recrystallization Textures, in Recrystallization and Related Annealing Phenomena*, 2nd Elsevier, Oxford.

15. Emren, F., Von, Schlippenbach, U. and Lucke, K. (1986). Investigation of the development of the recrystallization textures in deep drawing steels by ODF analysis. *Acta metal.* **34** : 2105-2117.

16. Chen, R., Zavalij, P. Y., Whittingham, M.S., Raju, N.P. and Bieringer, M. (1999). The hydrothermal synthesis of the new manganese and vanadium oxides, NiMnO3H, MAV3O7 and MA0.75V4O10·0.67H2O (MA = CH3NH3). *J. Mater. Chem.* **9** : 93-100.

17. Samajdar, I., Verlinden, B., Van Houtte, P. and Vanderschueren, D. (1997). γ-Fibre recrystallization texture in IF-steel: an investigation on the recrystallization mechanisms. *Mater. Sci. Eng. A.* **238(2)** : 343-350.

18. Hutchinson, W. B. (1989). Recrystallisation textures in iron resulting from nucleation at grain boundaries. *Acta Metall.* **37(4)** : 1047-1056.

19. Juntunen, P, Raabe, D., Karjalainen, P., Kopio, T. and Bolle, G. (2001). Optimizing continuous annealing of interstitial - free steels for improving deep drawability. *Metall. Mater. Trans. A.* **32(8)** : 1989-1995.

20. Park, Y.B., Lee, D. N. and Gottste, G. (1996). Development of texture inhomogeneity during hot rolling in interstitial free steel. *Acta Mater.* **44(8)** : 3421-3427.

21. Kestens, L. and Jonas, J. J. (1997). Modelling texture change during the static recrystallization of a cold rolled and annealed ultra low carbon steel previously warm rolled in the ferrite region. *ISIJ Int.* **37(8)** : 807-814.

22. Humphreys, F. J. (2001). Review : Grain and subgrain characterization by electron backscatter diffraction. *J. Mater. Sci.* **36(16)** : 3833-3854.